Copyright © 2004 Tech Science Press MCB, vol.1, no.4, pp.253-265, 2004

Force-induced Unfolding of the Focal Adhesion Targeting Domain and the Influence of Paxillin Binding

M.R. Kaazempur Mofrad[1,2], J. Golji[2], N.A. Abdul Rahim[2], R.D. Kamm[3]

Abstract: Membrane-bound integrin receptors are linked to intracellular signaling pathways through focal adhesion kinase (FAK). FAK tends to colocalize with integrin receptors at focal adhesions through its C-terminal focal adhesion targeting (FAT) domain. Through recruitment and binding of intracellular proteins, FAs transduce signals between the intracellular and extracellular regions that regulate a variety of cellular processes including cell migration, proliferation, apoptosis and detachment from the ECM. The mechanism of signaling through the cell is of interest, especially the transmission of mechanical forces and subsequent transduction into biological signals. One hypothesis relates mechanotransduction to conformational changes in intracellular proteins in the force transmission pathway, connecting the extracellular matrix with the cytoskeleton through FAs. To assess this hypothesis, we performed steered molecular dynamics simulations to mechanically unfold FAT and monitor how force-induced changes in the molecular conformation of FAT affect its binding to paxillin.

1 Introduction

Focal adhesion kinase (FAK) is an intracellular non-receptor protein tyrosine kinase that plays a critical role in linking membrane-bound integrin receptors to intracellular signaling pathways. In adherent cell types, FAK colocalizes with integrin receptors at focal adhesions (FA) through its C-terminal focal adhesion targeting (FAT) domain [Hayashi, Vuori, and Liddington (2002), Hildebrand, Schaller, and Parsons (1993)]. Focal adhesions, as sites of adhesion between cells and the extracellular matrix (ECM), allow ECM proteins to interact with membrane-bound receptors. Through recruitment and binding of intracellular proteins, FAs transduce signals across the cell membrane that regulate a variety of cellular processes including migration, proliferation, apoptosis and detachment from the ECM [Cary and Guan (1999), Hildebrand, Schaller, and Parsons (1993), Katz, Romer, Miyamoto, Volbert, Matsumoto, Cukierman, Geiger, and Yamada (2003), Liu, Guibao, and Zheng (2002), Parsons, Martin, Slack, Taylor, and Weed (2000), Zachary (1997)]. Signal transduction through FAs occurs via an elaborate and complex signaling network, involving multiple proteins, that is not entirely understood [Zamir and Geiger (2001)]. A schematic of this network is shown in Figure 1. FAK has been recognized as one of the critical proteins within this network that is activated by integrin signaling [reviewed in Schlaepfer, Hauck, and Sieg (1999), Shen and Schaller (1999)]. Aberrant FAK signaling, on the other hand, may contribute to the process of cell transformation by certain oncoproteins, thus leading to tumor progression and cancer development [Giancotti and Ruoslahti (1999), Jones, Machado, and Merlo (2001)].

The mechanism of signaling through and within the cell is of interest, especially the transmission of mechanical signals and subsequent transduction into biological and physiological signals. This transformation of signals, termed "mechanotransduction", is one of the signaling pathways available to cells as can be seen, for example, from the progression of arterial disease due to variations in fluid dynamic and solid stresses within vascular wall tissues. Various mechanisms have been proposed to explain this phenomenon. Some studies have suggested that a change in membrane fluidity acts to increase receptor mobility, leading to enhanced receptor clustering and signal initiation [Butler, Norwich, Weinbaum, and Chien (2001), Haidekker, L'Heureux, and Frangos (2000), White, Haidekker, Bao, and Fran-

[1] Current Address: Department of Bioengineering, University of California, Berkeley, CA

[2] Department of Mechanical Engineering and Biological Engineering Division, Massachusetts Institute of Technology, Cambridge, MA

[3] Department of Mechanical Engineering and Biological Engineering Division, Massachusetts Institute of Technology, 500 Technology Square, Room NE47-321, Cambridge, MA 02139, Email: rdkamm@mit.edu

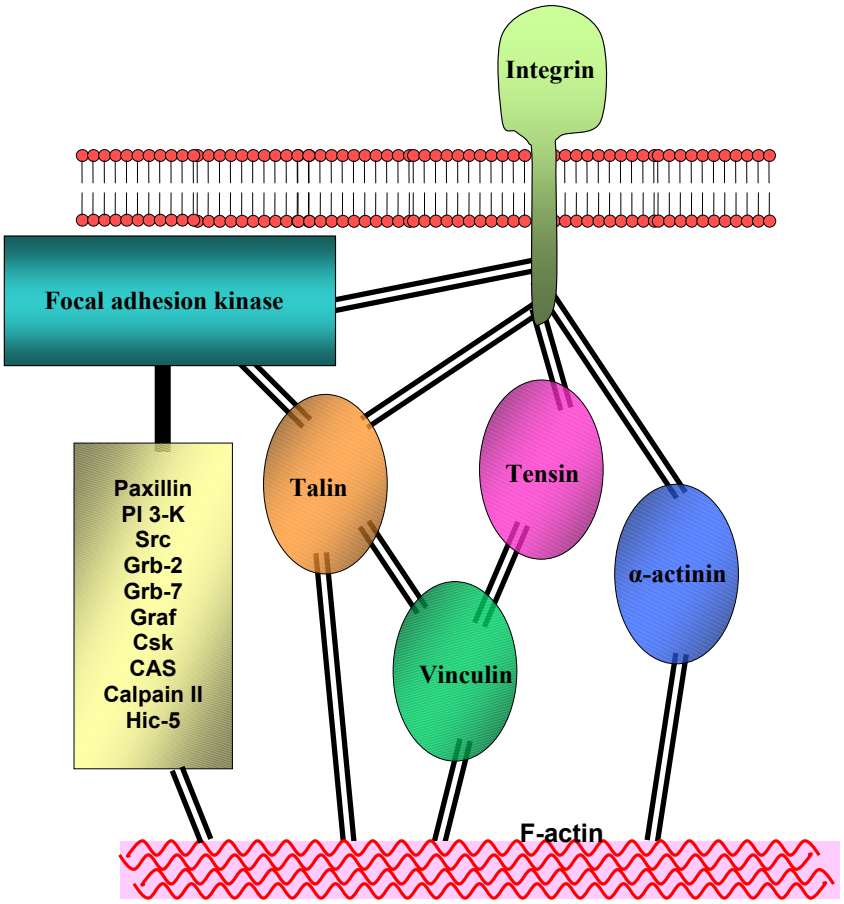

Figure 1 : Schematic representation of the many proteins involved in the complex signaling network that facilitates integrin-mediated signal transduction.

gos (2001)]. Stretch-activated ion channels represent a second means of mechanotransduction [Hamill and Martinac (2001)]. Mechanical disruption of microtubules [Odde, Ma, Briggs, DeMarco, and Kirschner (1999)] or forced deformations within the nucleus [Maniotis, Chen, and Ingber (1997)] have also been proposed. Constrained autocrine signaling is yet another mechanism whereby the strength of autocrine signaling is regulated by changes in the volume of extracellular compartments into which the receptor ligands are shed [Tschumperlin, Dai, Maly, Kikuchi, Laiho, McVittie, Haley, Lilly, So, Lauffenburger, Kamm, and Drazen (2004)]. Changing this volume by mechanical deformation of the tissues can increase the level of autocrine signaling. Finally, others have proposed conformational changes in intracellular proteins in the force transmission pathway connecting the extracellular matrix with the cytoskeleton through FAs as the main mechanotransduction mechanism [Helmke, Rosen, and Davies (2003), Sawada and Sheetz (2002), White, Haidekker, Bao, and Frangos (2001)].

We are interested in examining this last hypothesis regarding the effects of force-induced conformational change on a protein's biological function. Some proteins exist in a 'closed' structure that when triggered by force application, 'open up' to reveal cryptic binding clefts. An example of this is the formation of fibronectin fibrils through stretching of individual fibronectin molecules [Geiger and Bershadsky (2002)]. In a more subtle case, small conformational changes might also change binding affinity or enzyme activity. Tyrosine phosphorylation can modify a protein's structure and serve as receptors that recruit other molecules as occurs in the PDGF receptor. Where protein binding occurs through hydrophobic site interactions, a conformational change could modify this

function and potentially disrupt it totally. The FAT domain of FAK is one candidate for testing the conformational change hypothesis as it is an important signaling protein through its binding with paxillin and also has the potential to physically link integrins in the cell membrane to the cytoskeleton and thereby may be subject to conformational change as a consequence of externally-applied force.

The ∼150-residue region termed FAT resides within the C-terminal region of FAK. It is organized into four alpha-helix bundles of dimensions 60Å x 20Å x 20Å as shown in Fig. 2(a), with the helices straight, closely antiparallel and connected by short ordered turns. The bundle is highly compact and symmetrical with a square cross-section and a hydrophobic core known to be highly conserved across all species [Hayashi, Vuori, and Liddington (2002)]. Hydrophobic patches, HP1 and HP2, are located on the exposed faces of helix2-helix3 (Hx2-Hx3) and helix1-helix4 (Hx1-Hx4), respectively, as shown in Figure 2(b).

Paxillin (Pax) is a 559 amino acid adapter protein with an apparent molecular weight of 68kDa [Tumbarello, Brown, and Turner (2002)]. Within its N-terminal region are five distinct leucine-rich LD motifs of sequence LDXLLXXL, (Fig. 2(c)), each of which form individual amphipathic α-helices with minimal propensity to form secondary structures [Brown, Curtis, and Turner (1998)]. Two of these motifs, LD2 and LD4, have been found equally capable of binding to either HP1 or HP2, though segments containing both LD motifs bind 5-10 times stronger than those containing only one [Hayashi, Vuori, and Liddington (2002)].

Mutagenesis studies have shown that residues 919 – 1042 of FAT that form the 4-helix bundle are required in paxillin binding [Hayashi, Vuori, and Liddington (2002)]. This suggests that for hydrophobic binding of FAT-Pax to occur, the integrity of the helical bundle is required for conservation of the hydrophobic patches. Using this to test the hypothesis that cell signaling is controlled by force-induced conformational change of intracellular proteins, we apply mechanical force on a single FAT molecule and examine the effects of the resulting distortion of HP1 and HP2 hydrophobic patches, brought about through this conformational change, on its binding affinity to paxillin. We utilize the tools available through molecular dynamics (MD) and steered molecular dynamics (SMD) to apply a directed force and to monitor FAT's structural integrity. We demonstrate through the results of this force application, that the FAT-Pax complex is much more stable (requires larger force to unravel) than unbound FAT. Below, we first introduce the simulation methods, provide then a detailed comparison of trajectories and finally discuss the implications of our findings.

2 Methods

The coordinates of the unbound FAT (nb-FAT) crystal structure and the complex of the FAT molecule bound to the LD motif of paxillin (FAT-Pax) as determined by Hayashi et al. (2002) [Hayashi, Vuori, and Liddington (2002)] (Protein Data Bank entry code 1K40 and 1KKY, respectively) were used for computation. This complex involves a theoretical model with hypothetical LD motif peptides. For FAT-Pax, we examined the structure consisting of LD bound to HP1. Residues were renumbered 1-126 for FAT and 1-16 for the LD motif. The atomic structure of FAT is shown in Fig. 3(a) and in a 'tube' representation going through C-α backbone atoms in Fig. 3(b). The atomic structure of the FAT-Pax complex is shown in Fig. 3(c) where paxillin is highlighted, and in Fig. 3(d) in a 'tube' representation and colored pink. A close-up of paxillin on the FAT Hx2-Hx3 face is shown in Fig. 3(e), where residues forming salt bridges between the two motifs are colored blue and red, respectively.

Molecular dynamics (MD) calculates the time-dependent behavior of the molecular system by solving Newton's equation of motion for all atoms. In all simulations described here, computation was carried out with a commercially available software package CHARMM version c27b [Brooks, Bruccoleri, Olafson, States, Swaminathan, and Karplus (1983), MacKerell, Brooks, Brooks, Nilsson, Roux, Won, and Karplus (1998)], with top19.rtf and param19-1.2.prm CHARMM topology and parameter files for the empirical potential energy function.

All MD computations presented here were carried out using the analytical continuum electrostatics (ACE) potential implicit solvation model developed by Schaefer and Karplus [Schaefer and Karplus (1996)]. In this model, the solvent environment is approximated as a dielectric continuum where both the electrostatic, G^{el}, as well as non-polar, G^{np}, (non-electrostatic) solvation free energies contribute to the effective (free) energy, $G_{solvent}$, as

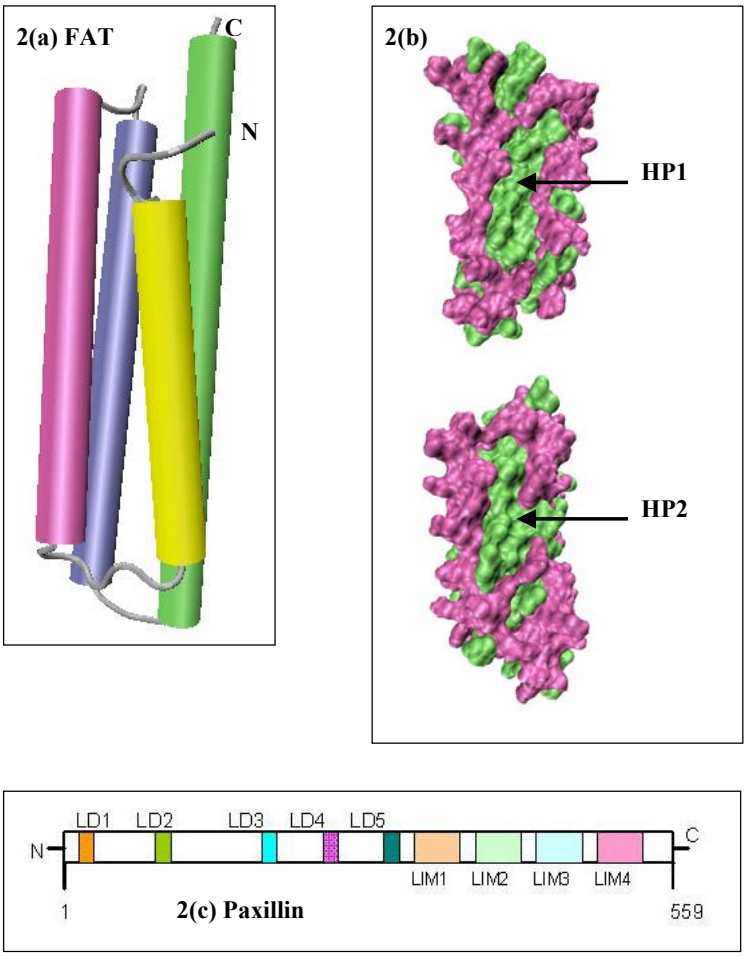

Figure 2 : (a) FAT: Four compact alpha-helical bundles. Straight, antiparallel and connected by short, ordered turns. 60Å long with a square cross-section of dimensions 20° x 20Å. (b) FAT: molecular surface showing hydrophobic patches, HP1 and HP2. Top: as seen in 2(a), but rotated 90° anti-clockwise about a vertical axis running through the 4-helix bundle. Bottom: as seen in 2(a), but rotated 90° clockwise about the vertical axis running through the 4-helix bundle. (c) Paxillin: positions of LD and LIM domains.

shown in Eq.1.

$$G_{solvent} = G^{el} + G^{np} \tag{1}$$

The first (electrostatic) contribution (G^{el}) is calculated using an analytical approximation to the solution of the Poisson's equation (ACE). The non-polar solvation free energy (G^{np}) is approximated by a pairwise potential.

For all MD simulations, an integration time step of 1fs was used and the ACE parameters were IEPS 1.0 (dielectric constant for space occupied by the molecule), SEPS 80.0 (dielectric constant for the solvent that is treated as a continuum), ALPHA 1.2 (Gaussian density distribution used to determine atom volume) and SIGMA 3.0 (scaling value for hydrophobic contribution to ACE). Non-bonded van der Waals and electrostatic interactions were treated with cut-off by using a switching function between 6.5Å and 7.5Å. The system contained a total of 1351 atoms.

Initially, the system was minimized using the Adopted Basis-set Newton-Raphson (ABNR) method for 1000 steps with no atoms fixed, to a sufficient GRMS of 0.32. Since the initial coordinates obtained from the crystal structure typically tend to have bad contacts that cause high energies and forces, the minimization process is needed to find a nearby local minimum. The system was then heated up gradually to 310K in 1000 steps and equi-

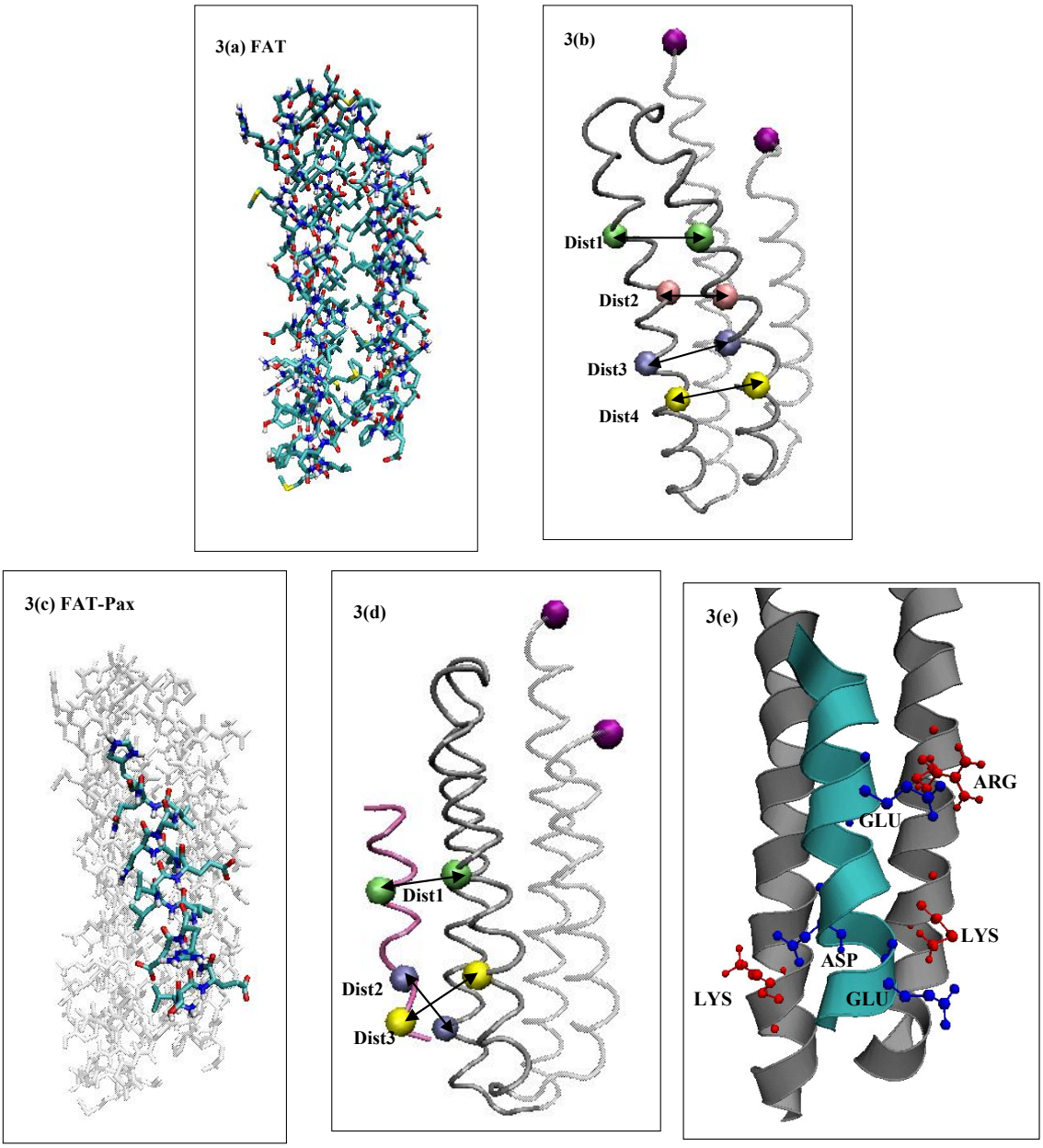

Figure 3 : (a) Atomic structure of FAT. As seen in Fig. 2(a), but rotated 90° anti-clockwise about a vertical axis running through the 4-helix bundle. (b) FAT in 'tube' representation. Hx1 and Hx 4 are colored lighter gray than Hx2 and Hx3. The termini C-α atoms are shown as magenta vdW spheres while the green, pink, blue and yellow spheres indicate the pairing between C-α hydrophobic atoms used in tracking the unraveling of FAT throughout SMD. (c) Atomic structure of FAT-Pax. FAT is colored gray and paxillin, according to the atoms in the LD motif. As seen in Fig. 2(a), but rotated 90° anti-clockwise about a vertical axis running through the 4-helix bundle. (d) FAT-Pax complex. The termini C-α atoms are shown as magenta vdW spheres while the green, blue and yellow spheres indicate the pairing between LD C-α atoms and FAT C-α atoms that form salt bridges between the motifs and which are tracked throughout the unraveling of FAT-Pax throughout SMD. (e) Paxillin (turquoise) on the Hx2-Hx3 face of FAT (gray). Residues forming salt bridges between the two motifs are shown in blue and red in 'ball-and-stick' representation for paxillin and FAT, respectively.

librated for 1000 steps until the energy was equally distributed throughout the molecule and the structure was stable. The equilibration process helps escape local minima with low energy barriers. Basic MD simulations effectively sample thermally accessible states within the energy landscape.

With temperature maintained at 310K, the N-terminal C-α atom was fixed and a constant force was applied to the C-terminal C-α atom. The force was applied in the normal direction away from the N-terminal C-α atom. Due to lack of actual, physiological data about the force configuration experienced by FAT in vivo, this arbitrary end-to-end pulling direction was deemed suitable for perturbing the molecular conformation and examining the mechanics of FAT. Such steering forces (hence, steered molecular dynamics—SMD) help access intermediate states that are not attained in a conventional MD on a reasonable time scale [Israelewitz, Baudry, Gullingsrud, Kosztin, and Schulten (2001)]. Constant-force SMD simulations were carried out for both unbound FAT (nb-FAT) and FAT complexed with the LD motif of paxillin (FAT-Pax) at different force levels until complete unfolding occurred. Unfolding is defined here as complete unraveling and straightening of the FAT bundle, which corresponds to an end-to-end distance of $\sim$400Å. The simulations presented here are referred to either as nb-FAT(force value) or FAT-Pax(force value) e.g. nb-FAT(75pN) or FAT-Pax(85pN). Levels of applied force were chosen so as to produce unraveling within a computationally reasonable timeframe $\sim$10 ns.

The analysis of SMD trajectories was conducted using a molecular visualization software VMD [Humphrey, Dalke, and Schulten (1996)]. The change in the end-to-end distance between the two termini C-α atoms of FAT is used as an indicator of progress of the unfolding process.

3 Results

3.1 Unraveling nb-FAT

SMD simulations with constant applied force, implemented in CHARMM, were carried out to probe the structural stability of isolated FAT in a solvated environment. Since the current region of interest for paxillin binding is hydrophobic patch 1 (HP1) formed at the interface between Hx2 and Hx3 (see Figure 2(b)), this binding site integrity was defined in terms of helix-to-helix separation. This separation was monitored through the distance analysis of four pairs of hydrophobic C-α atoms on the backbones of Hx2 and Hx3, respectively. This pairing is shown in Figure 3(b) as Ala46-Met65 (green), Leu41-Leu70 (pink), Gly38-Gly75 (blue) and Val34-Ile78 (yellow) where the C-α atoms were drawn in spherical van der Waals (vdW) representation. These distances are termed Distance 1, Distance 2, Distance 3 and Distance 4 respectively.

The unfolding trajectory of nb-FAT at an applied force of 75pN is shown in Figure 4, where both the end-to-end distance history and time snapshots of the molecule are presented at the corresponding intermediate stable structures. The end-to-end distance is shown by the black line and the four C-α atom pair distances are matched with their vdW pairing colors. As depicted in the figure, FAT was unraveled with a 75pN constant force from its equilibrated structure to its fully elongated configuration. Full unraveling occurs over 8ns during which ten plateau regions can be observed, indicating that the structure exhibits ten stable intermediate conformations before it fully unfolds. A sequence of unfolding snapshots is shown in Fig. 4(b) where each conformation corresponds to the plateau regions similarly labeled. It can be seen that the Hx2-Hx3 link is the first to unravel (Fig. 4(b)-C), which causes Distance 1 to be higher than the other inter-helix distances throughout conformations C-F, as this pair of C-α atoms are closest to the Hx2-Hx3 link. The top of Hx3 then unravels, followed by Hx1 (Fig 2(b)-D) and subsequently the other helixes. Even though Hx2 becomes severely distorted, it is the last to unravel (Fig. 2(b)-G). HP1 loses integrity after 4ns, corresponding to intermediate G where Hx2 has completely unraveled and so is no longer able to pair up with Hx3 to form HP1.

To examine the effect of force level on structural stability, unraveling was also computed for a force of 90pN and 100pN (data not shown). The unfolding pathways for both 90pN and 100pN simulations were similar, experiencing few short-lived stable intermediates before complete unraveling. Comparing the unraveling profile for the first 250ps of 90pN and 100pN simulations revealed that complete unraveling occurs slower for a lower applied force: in 225ps with 90pN compared to 70ps with a 100pN force. Loss of HP1 integrity occurred earlier compared to nb-FAT(75pN), at 150ps and 45ps for nb-FAT(90pN) and nb-FAT(100pN), respectively.

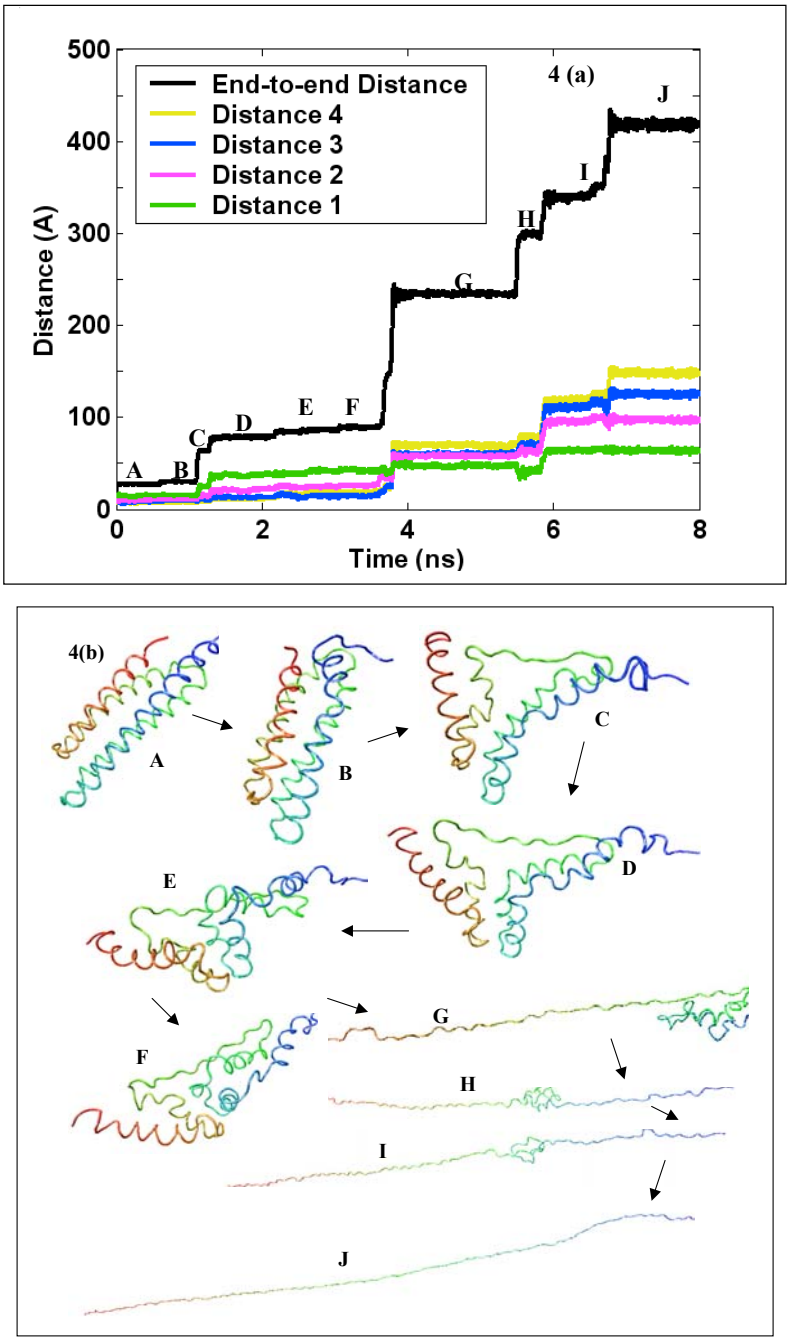

Figure 4 : (a) Distance *versus* time profile for nb-FAT(75pN) in water. (b) Sequence of unfolding conformations corresponding to the stable plateaus of Fig. 4(a). FAT is shaded red to blue from the C-terminal to the N-terminal.

3.2 Unraveling FAT-Pax

The unfolding pathways of FAT bound to the LD motif of paxillin (FAT-Pax complex) was studied with special attention to the influence of FAT's structural conformational change on its binding affinity with paxillin. The FAT termini end-to-end evolution was monitored under the application of force, as well as the binding affinity between FAT and paxillin. Binding affinity is denoted here as the distance between the following three pairs of C-α atoms on FAT and LD motif of paxillin, respectively, that form salt bridges: Arg42-Glu10 (green),

Lys82-Asp5 (blue) and Lys35-Glu3 (yellow), as shown in Fig. 3(c) where the C-α atoms were drawn in spherical vdW representation and these distances are termed Distance 1, Distance 2 and Distance 3 respectively.

Unlike the case with unbound-FAT, the FAT molecule bound to paxillin did not unravel with application of a 75pN force (see Fig. 5(a)). This implies that binding with paxillin increases the structural stability of FAT. Applied forces were subsequently increased to 85pN (see Fig. 5(b)) and larger forces up to 200pN (data not shown). 85pN was the lowest force required to produce unraveling within a computationally accessible time frame, where FAT-Pax unraveling occurred within 2ns, having gone through two stable intermediate structures. For subsequent higher forces, unraveling proceeds relatively smoothly without any clearly delineated stable intermediate structures. For all trajectories, the unfolding pathway exhibits prolonged binding between FAT-Pax where the binding site is maintained and is one of the last motifs to unravel. As FAT unfolds, helix 2 and helix 3 remain intact and simulations determined that the salt bridge between Lys82-Asp5 is what keeps paxillin bound to FAT and is the last bond to be broken. Once this bond is broken, FAT completely unravels.

Increased force levels reduced the unfolding time, e.g. from 2ns for 85pN down to 35ps for 200pN. With 85pN, 100pN and 125pN, the force level was high enough to unravel FAT but not sufficient to completely remove paxillin from the system and the distances between FAT-Pax C-α atoms remain below 200Å (Fig. 5(b)). This is in contrast to both the FAT-Pax(150pN) and FAT-Pax(200pN) cases where paxillin is released from the system.

4 Discussion

Mechanical unfolding of FAT, both isolated and bound to paxillin, were carried out to monitor how changes in the molecular conformation of FAT, induced by direct application of force, would affect its binding with paxillin. Several noteworthy points were observed regarding the integrity and stability of the FAT structure, how it is influenced by force application, and its impact on FAT-Pax binding affinity.

4.1 Force-dependence of Unfolding Pathways

FAT exhibits different unfolding pathways depending on the magnitude of applied force. At 75pN, more intermediate stable conformations are sampled (ten intermediaries) compared to when higher forces are applied. A schematic description of force-induced variation in the protein energy landscape is given in Figure 6. The energy landscape of the initial structure, with no perturbation added to the system, is represented by the solid black curve in the figure. Valleys correspond to stable intermediate structures and are labeled A, B, C, D according to the stable intermediaries observed from nb-FAT(75pN) whereas hills are energy barriers that have to be overcome in order to access the adjacent stable intermediaries. The application of force subtracts an ever-increasing energy component, *Fx*, here presented as dashed lines, which distorts the energy landscape and tilts it downwards. With 75pN applied force, *Fx* is shown by the dashed red line. The tilt in the energy landscape, represented by the solid red line, reduces the energy required to overcome barriers but preserves all the minimum-energy valleys. Thus the stable intermediate conformations are still seen in the SMD simulation and all A, B, C, D valleys are present. When higher forces are applied, the degree of tilting increases and some of the valleys are eliminated, as is represented by the green and blue solid lines for 90pN and 100pN respectively. 90pN eliminates the last valley, leaving only A, B and C while 100pN eliminates one more than that, leaving A and B. Admittedly, energy landscapes correspond to the free energy states of the molecule and therefore cannot be used as a rigorous representation of our system, as force application in the way we have introduced here does not maintain the system at equilibrium. However, the energy landscape provides a useful qualitative understanding of the unfolding trajectories.

4.2 Unbound and Bound FAT Unfold Differently

The lowest force level, 75pN, represented our computational limit and produced nb-FAT(75pN) unraveling within 8ns. However, FAT-Pax(75pN) did not produce similar unraveling, as shown in the comparison in Fig. 5(a). This indicates that paxillin binding increases the structural strength and stability of FAT, and therefore increases the unfolding threshold.

For nb-FAT, the two hydrophobic patches HP1 and HP2 are exposed to the solvated environment. Hydrophobic

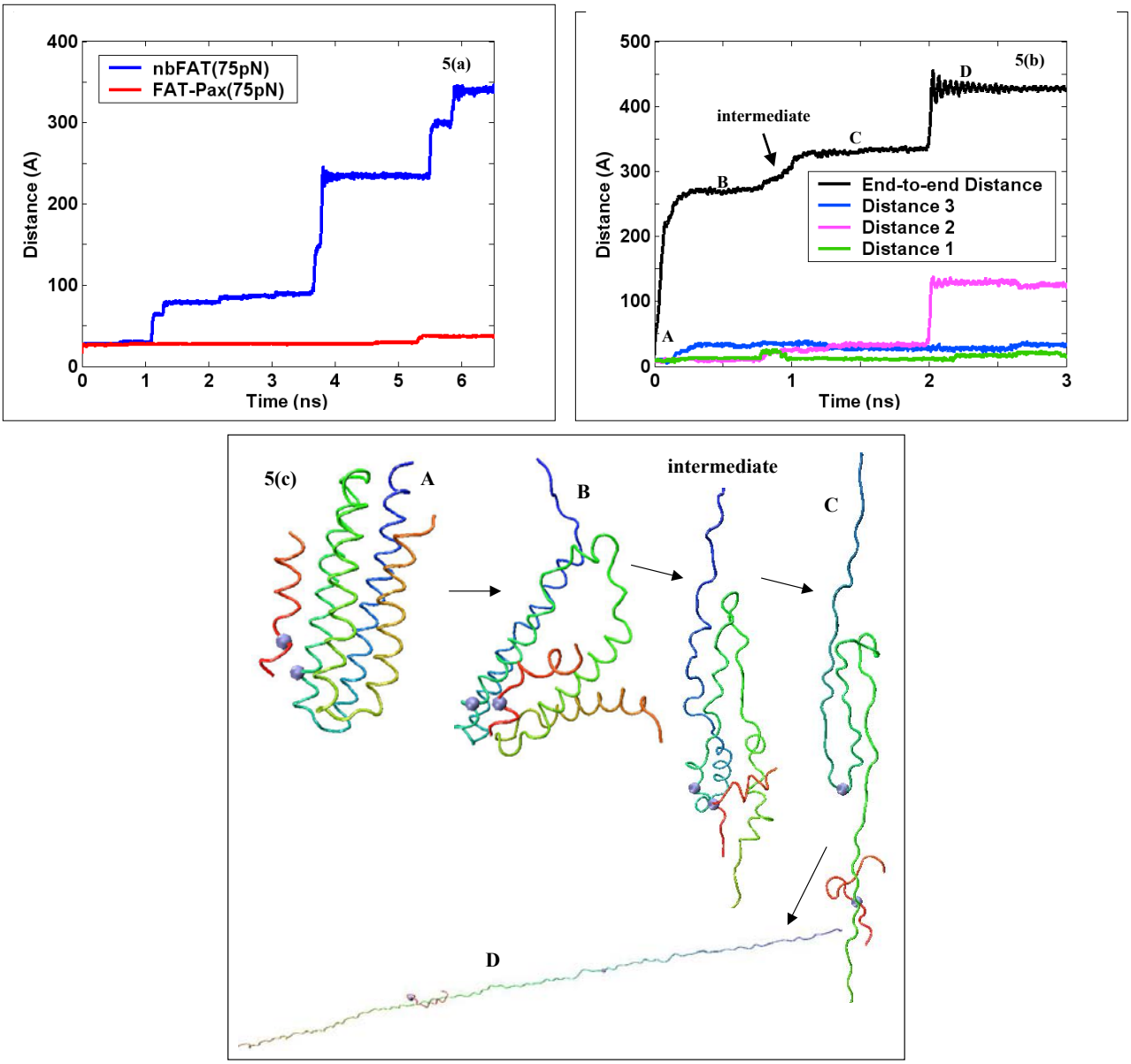

Figure 5 : (a) Comparison between nb-FAT(75pN) with FAT-Pax(75pN) unraveling profile, both in water. (b) Distance *versus* time profile of FAT-Pax(85pN) in water (c) Sequence of unfolding conformations for FAT-Pax. FAT is shaded red to blue from the C-terminal to the N-terminal.

residues have low affinity for water and hence these hydrophobic patches on the surface provide minimal stability, if any, to the 4-helix FAT bundle. Binding of the LD motif of paxillin as in the FAT-Pax complex would thus increase FAT stability as it results in HP1 becoming buried between the two domains. This increase in stability is reflected in the increased applied forces needed to overcome the FAT-Pax unraveling threshold.

4.3 Unfolding Pathway

Even though the unfolding pathway sampled by nb-FAT and FAT-Pax differed substantially (see Figs. 4(b) and 5(c)), both progressed in a manner that kept the hydrophobic groove HP1 intact. To further examine this behavior and ensure that it is not an artifact of the implicit solvent model, we carried out preliminary SMD simulations of FAT-Pax in an explicit solvation model

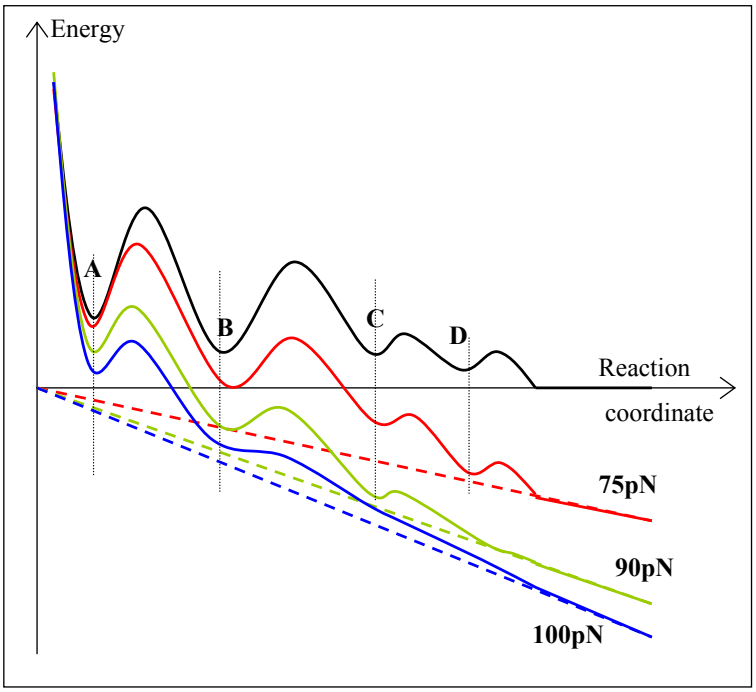

Figure 6 : Schematic description of force-induced variation in the FAT energy landscape. Solid lines: energy landscape. Dashed lines: *-Fx* for three levels of force.

incorporating TIP3P water box with periodic boundary conditions. The water box was of dimension 70Å x 70Å x 270Å and the system contained more than 150,000 atoms. Even though full unraveling of FAT was not achieved during this run due to prohibitive computing costs, initial observations were in qualitative agreement with the results obtained with implicit solvent model.

Our results support the speculation that the integrity of FAT, especially the conformation of the hydrophobic groove HP1, is crucial for its binding to paxillin [Hayashi, Vuori, and Liddington (2002)]. With the distortion of this hydrophobic patch, the LD motif of paxillin is unable to align with the hydrophobic groove HP1 and FAT-Pax binding cannot occur. Since the SMD simulations of nb-FAT and FAT-Pax, using both implicit and explicit water models, showed that HP1 is kept intact and is the last to unravel, this supports the concept that the FAT molecular structure is such that the HP1 binding site is maintained as long as possible even when subjected to adverse conditions, as represented here by a high and prolonged force application to the ends of FAT. This also indicates that the formation of the FAT 4-helix bundle through alignment of its particular set of amino acids is optimized for promoting the paxillin binding event. The initial hypothesis that the entire helix bundle is necessary for paxillin binding can therefore be refined to the suggestion that it is only the helical binding face, HP1, that needs to be intact for paxillin binding.

It should be noted that HP2 also exists on the face of Hx1-Hx4. The nature of our force application direction results in immediate destruction of this hydrophobic patch. It is conceivable that should the force application be modified to include for example shearing of Hx2-Hx3 relative to Hx1-Hx4, both patches would be intact and analysis can then be done through SMD on the effect of having an LD-motif on one face and no LD-motif on the other face. We should observe that the face lacking an LD-motif would lose stability before the LD face does. More generally, caution should be used in applying these results to forces applied at different locations and along different directions.

4.4 Physiological Relevance

Our SMD simulations are restricted to a few nanoseconds due to the constraint presented by current computational resources. In order to produce unraveling events

that occur fast enough to be observed within these simulations, forces of 75pN and higher had to be used. Experiments, meanwhile, have shown that concentrated apical cell surface loads of ∼10nN initiate focal adhesion complex formation and protein recruitment along the basal cell surface in regions local to the concentrated load [Riveline, Zamir, Balaban, Schwarz, Ishizaki, Narumiya, Kam, Geiger, and Bershadsky (2001)]. Also, nN level forces applied to the apical cell surface induce translocation of FAs [Mack, Kaazempur-Mofrad, Karcher, Lee, and Kamm (2004)]. Both these experiments implicate force levels of hundreds of pN per FA and thus a few pN per integrin, to which FAT is connected as being important biologically. Our applied force levels would therefore appear too high in comparison. This can be resolved by understanding that the force magnitudes necessary to produce effects on molecules depend on the loading rate [Evans and Ritchie (1997)]. Within cells, the magnitude of a few pN forces experienced, caused either externally by arterial shear stress and solid dynamics or internally through cytoskeleton reorganization, occurs over a matter of milliseconds to seconds. This is equivalent to a very slow loading rate. For our simulations however, the short simulation times imposed by the limitations of computer resources requires that FAT be stretched at forces one to two orders of magnitude higher than forces present in the cellular environment. In SMD simulations, the forces applied tilt energy landscapes, reduce energy barriers and are large enough to then overcome those smaller barriers that remain.

5 Outlook

The main shortcoming of the present investigation is the overestimation of the unraveling force and the degree of unraveling required for HP1 disruption. It is highly unlikely that physiological-level forces would be applied for a sufficiently long time to cause such complete unraveling within the cell. We have started investigations into other more physiologically relevant conformational changes that could occur to the FAT domain.

Normal mode analysis (NMA) has proven to be useful for identifying collective domain motions of proteins [Brooks and Karplus (1985), Marques and Sanejouand (1995), Tama and Sanejouand (2001)]. Some of the lowest-frequency normal modes of several proteins correlate well with the proteins' conformational change. NMA can therefore be carried out on the 4-helical FAT bundle, where the protein is modeled as a collection of masses (atoms) and springs (interactions) and all specific electrostatic and van der Waals forces are ignored. Starting from a state of minimum energy (energy well), instead of accounting for all bonded and non-bonded forces, the molecular potential energy can be approximated as a harmonic function (Hookean potential). Using this approximation, the normal modes of motion are calculated. The modes with lowest frequencies would correspond to conformational changes more physiologically relevant and accessible to the FAT bundle. Thereafter, using SMD, forces can be applied that would stimulate this conformational change and subsequent bundle integrity as well as binding affinity can be observed.

Even with the shortcomings mentioned, the present work demonstrates that force-induced conformational change in individual proteins is a highly plausible mechanism for transduction of mechanical signals carried via alteration of binding events in the mechanosensing pathways. Force application eventually remodeled the hydrophobic groove of FAT, affecting the FAT-Pax binding partnership. Putting this in the context of the cell, unbinding might in turn cause disruption of the downstream signaling pathway.

References

Brooks, B. R.; Bruccoleri, R. E.; Olafson, B. D.; States, D. J.; Swaminathan, S.; Karplus, M. (1983): CHARMM: A program for macromoleculary energy, minimization and dynamics calculations. *J Comp Chem* 4: 187-217.

Brooks, B.; Karplus, M. (1985): Normal modes for specific motions of macromolecules: application to the hinge-bending mode of lysozyme. *Proc Natl Acad Sci USA* 82(15): 4995-9.

Brown, M. C.; Curtis, M. S.; Turner, C. E. (1998): Paxillin LD motifs may define a new family of protein recognition domains. *Nat Struct Biol* 5(8): 677-8. Review.

Butler, P. J.; Norwich, G.; Weinbaum, S.; Chien, S. (2001): Shear stress induces a time- and position-dependent increase in endothelial cell membrane fluidity. *Am J Physiol Cell Physiol* 280: C962-9.

Cary, L. A.; Guan, J. L. (1999): Focal adhesion kinase in integrin-mediated signaling. *Front Biosc.* 4: D102-13. Review.

Cooley, M. A.; Broome, J. M.; Ohngemach, C.; Romer, L. H.; Schaller, M. D. (2000): Paxillin binding is not the sole determinant of focal adhesion localization or dominant-negative activity of focal adhesion kinase/focal adhesion kinase-related nonkinase. *Mol Biol Cell* 11(9): 3247-63.

Evans, E.; Ritchie, K. (1997): Dynamic strength of molecular adhesion bonds. *Biophys J* 72(4): 1541-55.

Geiger, B.; Bershadsky, A. (2002): Exploring the Neighborhood: Adhesion-Coupled Cell Mechanosensors. *Cell* 110: 139-142.

Geiger, B.; Bershadsky, A.; Pankov, R.; Yamada, K. M. (2001): Transmembrane crosstalk between the extracellular matrix—cytoskeleton crosstalk. *Nat Rev Mol Cell Biol* 2(11): 793-805.

Giancotti, F. G.; Ruoslahti, E. (1999): Integrin signaling. *Science* 285(5430): 1028-33.

Haidekker, M. A.; L'Heureux, N.; Frangos, J. A. (2000): Fluid shear stress increases membrane fluidity in endothelial cells: a study with DCVJ fluorescence. *Am J Physiol Heart Circ Physiol* 278: H1401-6.

Hamill, O. P.; Martinac, C. (2001): Molecular Basis of Mechanotransduction in Living Cells. *Physiol Rev* 81: 685-740.

Hayashi, I.; Vuori, K.; Liddington, R. C. (2002): The focal adhesion targeting (FAT) region of focal adhesion kinase is a four-helix bundle that binds paxillin. *Nat Struct Biol* 9(2):101-6.

Helmke, B. P.; Rosen, A. B.; Davies, P. F. (2003): Mapping mechanical strain of an endogenous cytoskeletal network in living endothelial cells. *Biophys J* 84:2691-99.

Hildebrand, J. D.; Schaller, M. D.; Parsons, J. T. (1993): Identification of sequences required for the efficient localization of the focal adhesion kinase, pp125FAK, to cellular focal adhesions. *J Cell Biol* 123(4): 993-1005.

Humphrey, W.; Dalke, A.; Schulten, K. (1996): VMD – Visual Molecular Dynamics. *J Molec Graphics* 14: 33-38.

Isralewitz, B.; Baudry, J.; Gullingsrud, J.; Kosztin, D.; Schulten, K. (2001): Steered molecular dynamics investigations of protein function. *J Mol Graphics and Modeling* 19: 13-25.

Jones, G.; Machado, J. Jr.; Merlo, A. (2001): Loss of focal adhesion kinase (FAK) inhibits epidermal growth factor receptor-dependent migration and induces aggregation of nh(2)-terminal FAK in the nuclei of apoptotic glioblastoma cells. *Cancer Res* 61(13): 4978-81.

Katz, B. Z.; Romer, L.; Miyamoto, S.; Volbert, T.; Matsumoto, K.; Cukierman, E.; Geiger, B.; Yamada, K. M. (2003): Targeting membrane-localized focal adhesion kinase to focal adhesions: roles of tyrosine phosphorylation and SRC family kinases. *J Biol Chem* 278(31): 29115-20.

Liu, G.; Guibao, C. D.; Zheng, J. (2002): Structural insight into the mechanisms of targeting and signaling of focal adhesion kinase. *Mol Cell Biol* 22(8): 2751-60.

MacKerell, A. D. Jr.; Brooks, B.; Brooks, C. L. III; Nilsson, L.; Roux, B.; Won, Y.; Karplus, M. (1998): CHARMM: The energy function and its parameterization with an overview of the program. *The Encyclopedia of Computational Chemistry*, 1:271-277, Schleger PVR et. al (eds.). Wiley: New York.

Mack, P. J.; Kaazempur-Mofrad, M. R.; Karcher, H.; Lee, R. T.; Kamm, R. D. (2004): Force-induced focal adhesion translocation: Effects of force amplitude and frequency. *Am J Physiol Cell Physiol*.

Maniotis, A. J.; Chen, C. S.; Ingber, D. E. (1997): Demonstration of mechanical connections between integrins, cytoskeletal filaments and nucleoplasm that stabilize nuclear structure. *Proc Natl Acad Sci USA* 94: 849-54.

Marques, O.; Sanejouand, Y. H. (1995): Hinge-bending motion in citrate synthase arising from normal mode calculations. *Proteins* 23(4): 557-60.

Merkel, R.; Nassoy, P.; Leung, A.; Ritchie, K.; Evans, E. (1999): Energy landscapes of receptor-ligand bonds explored with dynamic force spectroscopy. *Nature.* 397: 50-53.

Odde, D. J.; Ma, L.; Briggs, A. H.; DeMarco, A.; Kirschner, M. W. (1999): Microtubule bending and breaking in living fibroblast cells. *J Cell Sci* 112: 3283-8.

Parsons, J. T.; Martin, K. H.; Slack, J. K.; Taylor, J. M.; Weed, S. A. (2000): Focal adhesion kinase: a regulator of focal adhesion dynamics and cell movement. *Oncogene.* 19(49): 5606-13. Review.

Riveline, D.; Zamir, E.; Balaban, N. Q.; Schwarz, U. S.; Ishizaki, T.; Narumiya, S.; Kam, Z.; Geiger, B.; Bershadsky, A. D. (2001): Focal contacts as

mechanosensors: externally applied local mechanical force induces growth of focal contacts by an mDio1-dependent and ROCK-independent mechanism. *J Cell Biol* 153: 1175-86.

Sawada, Y.; Sheetz, M. P. (2002): Force transduction by Triton cytoskeletons. *J Cell Biol* 156: 609-615.

Schaefer, M.; Karplus, M. (1996): A comprehensive analytical treatment of continuum electrostatics. *J Phys Chem* 100: 1578-99.

Schlaepfer, D. D.; Hauck, C. R.; Sieg, D. J. (1999): Signaling through focal adhesion kinase. *Prog Biophys Mol Biol* 71(3-4): 435-78.

Shen, Y.; Schaller, M. D. (1999): Focal adhesion targeting: the critical determinant of FAK regulation and substrate phosphorylation. *Mol Biol Cell* 10(8): 2507-18.

Tama, F.; Sanejouand, Y. H. (2001): Conformational change of proteins arising from normal mode calculations. *Protein Eng* 14(1): 1-6.

Tschumperlin, D. J.; Dai, G.; Maly, I. V.; Kikuchi, T.; Laiho, L. H.; McVittie, A. K.; Haley, K. J.; Lilly, C. M.; So, P. T.; Lauffenburger, D. A.; Kamm, R. D.; Drazen, J. M. (2004): Mechanotransduction through growth-factor shedding into the extracellular space. *Nature* 429: 83-6.

Tumbarello, D. A.; Brown, M. C.; Turner, C. E. (2002): The paxillin LD motifs. *FEBS Lett* 513(1): 114-8.

White, C. R.; Haidekker, M.; Bao, X.; Frangos, J. A. (2001): Temporal gradients in shear, but not spatial gradients, stimulate endothelial cell proliferation. *Circulation* 103:2508-13.

Zachary, I. (1997): Focal adhesion kinase. *Int J Biochem Cel. Biol* (7): 929-34. Review.

Zamir, E.; Geiger, B. (2001): Components of cell-matrix adhesions. *J Cell Sci* 114(Pt 20): 3577-9.